ISSN: 0975-8585

Research Journal of Pharmaceutical, Biological and Chemical Sciences

Spectral, Magnetic, Thermal studies and Antimicrobial activity of (E)-3-(2-Benzylidenehydrazinyl)-3-OXO-N-(Thiazol-2-yl) Propanamide complexes

KM Ibrahim, RR Zaky*, EA Gomaa, MN El-Hady

Department of Chemistry, Faculty of Science, Mansoura University, Mansoura, Egypt

ABSTRACT

(*E*)-3-(2-benzylidenehydrazinyl)-3-oxo-*N*-(thiazol-2-yl) propanamide (H_2L) has been prepared and its structure confirmed by elemental analysis, IR and ^{1}H NMR spectroscopy. It has been used to produce diverse complexes with Ni(II), Co(II), Cu(II), Pd(II), Cd(II), Hg(II) and Zn(II) ions. The complexes obtained have been investigated by thermal analysis, spectral studies (IR, UV–visible, ^{1}H NMR), and magnetic measurements. IR spectra suggest that the H_2L acts as a bidentate and/or tridentate ligand. The electronic spectra of the complexes and their magnetic moments suggesting octahedral geometry for the isolated complexes. The molar conductance measurements proved that the complexes are non-electrolytes. Also, Thermal properties and decomposition kinetics of all compounds are investigated. The interpretation, mathematical analysis and evaluation of kinetic parameters (Ea, A, ΔH, ΔS and ΔG) of all thermal decomposition stages have been evaluated using Coats–Redfern method. Moreover, the antimicrobial activity has been tested.

Keywords*:* Hydrazone complexes; ^{1}H NMR; Thermal analysis; Anti-microbial.

Corresponding author

INTRODUCTION

The coordination chemistry of hydrazones has received much impetus by the remarkable anticancer, amoebicidal, antibacterial, antimicrobial and antileukaemic activities exhibited by these compounds which can be related to their metal complexing abilities [1-3]. Aroylhydrazone possess strong pharmacologial properties and may inhibit many enzymatic reactions catalysed by transition metals. The chemical and pharmacological properties of aroylhydrazone have been extensively investigated owing to their potential applications as antineoplastic, antiviral, antiinflammatory and antitumor agents [4-6]. Also, hydrazones have been used for the analytical determination of wide variety of metal ions [7-9]. Hydrazones have interesting ligation properties due to presence of several coordination sites. The metal complexes formed by the combination of transition metal ion with a potent acylhydrazone ligand should be more biologically active than the metal salts or the ligand individually. Therefore, we report here the synthesis and characterization of Ni(II), Co(II), Cu(II), Pd(II), Cd(II), Hg(II) and Zn(II) complexes with *(E)*-3-(2-(2hydroxybenzylidene)hydrazinyl)-3-oxo-n(thiazole-2-yl)propanamide (H_2L). The antifungal and antibacterial properties of the ligand and its complexes were tested.

EXPERIMENTAL

Apparatus and reagents

The IR absorption spectra were recorded on a Mattson 5000 FTIR Spectrophotometer. The electronic spectra were measured on a Unicam UV/vis Spectrometer UV_2. Thermogravimetric analysis was performed using an automatic recording thermobalance type (951 DuPont instrument). Samples were subjected to heat on a rate of 10 °C/min (25-800 °C) in N_2. ^{1}H NMR spectra for H_2L and diamagnetic complexes, in *DMSO*, were recorded on EM-390 (200 MHz) Spectrometer. Carbon and hydrogen content for the ligand and its complexes was determined at the Microanalytical Unit, Mansoura University, Egypt. Ni(II), Co(II), Cu(II), Pd(II), Cd(II), Hg(II) and Zn(II), Cl^- and $SO4^{2-}$ contents in the complexes were determined by the well known standard methods [10]. All metal salts used were pure (Fluka, Aldrich or Merck).

Preparation of the ligand

(*E*)-3-(2-(2-hydroxybenzylidene)hydrazinyl)-3-oxo-n(thiazole-2yl)propan -amide (Scheme 1) was prepared by heating a mixture of 3-hydrazinyl-oxo-*N*-(thiazole-2-) propanamide (0.01 mol; 2.00 g) and benzaldehyde (0.01 mol; 1.36 g) under reflux in absolute ethanol for 3 h. On cooling, white crystals were formed, filtered off, washed with EtOH and Et_2O and recrystallized from EtOH (M.p.: 225 ^oC; yield 90%). The purity of the compound was checked by TLC.

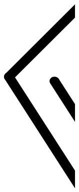

Scheme 1. The outline of the synthesis of ligand and its complexes.

Preparation of complexes

The complexes were prepared by mixing equimolar amounts of H_2L with ethanolic and/or aqueous solution of chloride salt of Cd(II) and pd(II) as potassium tetrachloropalladate; acetate salt of Ni(II), Co(II), Cu(II) and Zn(II) and sulphate salt of Cu(II). The reaction mixture was heated on a water bath for 1–3 h. The precipitate was filtered off, washed with hot EtOH and/or H_2O successfully and finally preserved in a vacuum desiccator over anhydrous $CaCl_2$.

Biological activity

Antifungal activity

The ligand H_2L as well as its metal complexes Ni(II), Co(II), Cu(II), Cd(II), Zn(II) and Pd(II) were screened for their antifungal activity against various fungi *viz*. *Aspergillus sp.*, and *Stemphylium sp.* These species were isolated from the infected organs of the host plants on potato dextrose agar (potato 250 g + dextrose 20 g + agar 20 g) medium. The cultures of the fungi were purified by single spore isolation technique. The solution in different concentrations 0.5, 1 and 1.5 mg/ml of each compound in *DMSO* were prepared for testing against spore germination. A drop of the solution of each concentration was kept separately on glass slides. The conidia, fungal reproducing spores (approximately 200) lifted with the help of an inoculating needle, were mixed in every drop of each compound separately. Each treatment was replicated thrice and a parallel *DMSO* solvent control set was run concurrently on separate glass slides. All the slides were incubated in humid chambers at 25 ± 2°C for 24 h. Each slide was observed under the microscope for spore germination and percent germination was finally calculated. The results were also compared with a standard antifungal drug *Miconazole* at the same concentrations.

Antibacterial activity

The antibacterial activity of the ligands H_2L and its metal complexes (Ni(II), Co(II), Cu(II), Hg(II), Cd(II), Zn(II) and Pd(II) were studied against *Clostridium sp.* and *E. Coli* bacteria. The solution in different concentrations 0.5, 1 and 1.5 mg/ml of each compound in *DMSO* were prepared for testing against spore germination. Paper discs of Whatman filter paper (No. 42) of uniform diameter (2 cm) were cut and sterilized in an autoclave. The paper discs soaked in the desired concentration of the complex solutions were placed aseptically in the petridishes containing nutrient agar media (agar 20 g + beef extract 3 g + peptone 5 g) seeded with Clostridium sp. and E. coli bacteria separately. The petridishes were incubated at 37°C and the inhibition zones were recorded after 24 h of incubation. The antibacterial activity of a common standard antibiotic *Ampicillin* was also recorded using the same procedure as above at the same concentrations and solvent. The results were also compared with a standard antibacterial drug *Ampicillin* at the same concentrations.

RESULTS AND DISCUSSION

Table (1): Analytical and physical data of H_2L and its metal complexes

Compound	Empirical Formula (F. Wt.)	Colour	M.P. (°C)	Yeild (%)	%Found (Calcd.)			
					C	H	M	X
H_2L	$C_{13}H_{12}O_2N_4S$ (288.203)	white	230	80	54.24 (54.13)	4.06 (4.19)	- -	-
$[Zn(H_2L)(OAc)_2].H_2O$	$ZnC_{17}H_{20}O_7N_4S$ (489.608)	yellow	> 300	70	41.45 (41.66)	4.15 (4.08)	13.37 (13.36)	-
$[Pd(H_2L)Cl_2].2H_2O$	$PdC_{13}H_{16}O_4N_4SCl_2$ (501.653)	Pale - yellow	262	85	31.29 (31.09)	3.03 (3.18)	21.34 (21.21)	14.20 (14.15)
$[Cu(H_2L)(SO_4)H_2O].H_2O$	$CuC_{13}H_{16}O_8N_4S_2$ (485.773)	Pale-green	> 300	80	35.09 (32.11)	3.48 (3.32)	13. 07 (13.01)	19.94 (20.18)
$[Cd(HL)Cl].H_2O$	$CdC_{13}H_{13}O_3N_4SCl$ (453.165)	red	280	79	34.36 (34.42)	3.05 (2.86)	24.17 (24.18)	7.67 (7.80)
$Ni(HL)(OAc)H_2O].2H_2O$	$NiC_{15}H_{20}O_7N_4S$ (458.995)	brown	> 300	85	39.29 (39.25)	4.26 (4.39)	12.89 (12.79)	-
$[Co(L)(H_2O)_3].H_2O$	$CoC_{13}H_{18}O_6N_4S$ (417.175)	brown	> 300	85	37.46 (37.39)	4.29 (4.35)	14.19 (14.13)	-
$[Cu(L)(H_2O)_3].H_2O$	$CuC_{13}H_{18}O_6N_4S$ (421.787)	green	> 300	78	37.09 (37.02)	4.28 (4.32)	15.14 (15.06)	-

The isolated solid complexes are stable in air and easily soluble in *DMF* and *DMSO*. The molar conductance values, in *DMSO*, is 3-6 $Ohm^{-1}cm^2mol^{-1}$ indicating that the all complexes are non-electrolytes Table 1.

IR and ^{1}H-NMR spectral studies

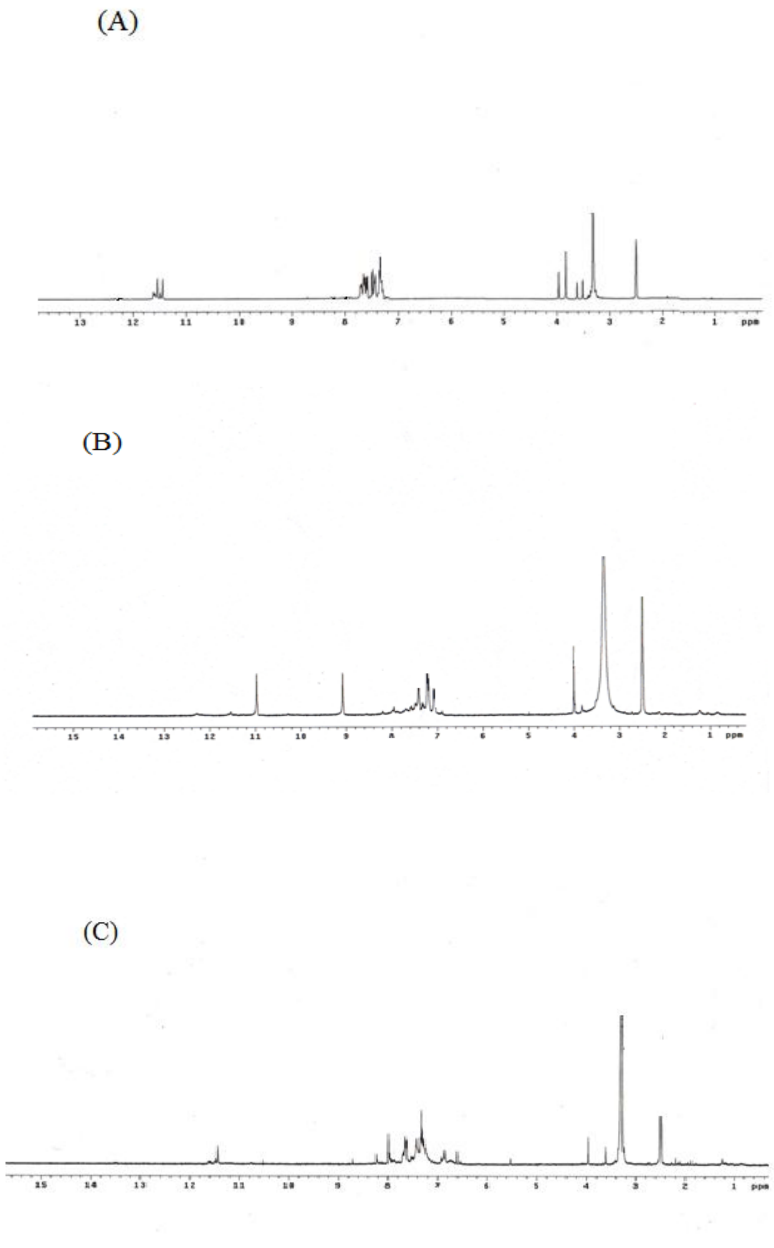

Fig. (1): ^{1}H NMR spectra of (A) (H_2L), (B) $[Pd(H_2L)Cl_2].2H_2O$ and (C) $[Cd(HL)Cl].H_2O$

Table (2): Most important IR spectral bands of H_2L and its metal complexes in cm^{-1}

Compound	υ $(NH)_1$	υ $(NH)_2$	υ $(C=O)_1$	υ $(C=O)_2$	υ (C=N)	$\upsilon(C=N^*)_1$	$\upsilon(C=N^*)_2$	υ $(C-O)_1$	υ $(C-O)_2$	υ(M-O)	υ(M-N)
H_2L	3282	3215	1688	1669	1615	-	-	-	-	-	-
$[Zn(H_2L)(OAc)_2].H_2O$	3256	3210	1666	1642	1621	-	-	-	-	495	-
$[Pd(H_2L)Cl_2].2H_2O$	3205	3170	1678	1659	1614	-	-	-	-	514	-
$[Cu(H_2L)(SO_4)H_2O].H_2O$	3214	3122	1671	1635	1589	-	-	-	-	514	440
$[Ni(HL)(OAc)H_2O].2H_2O$	-	3212	-	1646	1602	1623	-	1166	-	520	460
$[Cd(HL)Cl].H_2O$	-	3184	-	1656	1602	1624	-	1162	-	535	423
$[Co(L)(H_2O)_3].H_2O$	-	-	-	-	1593	1617	1615	1166	1112	516	470
$[Cu(L)(H_2O)_3].H_2O$	-	-	-	-	1590	1617	1615	1172	1112	510	450

The most important infrared bands of H_2L and its metal complexes are listed in Table 2 and represented graphically in Fig. 1.

The IR spectrum of H_2L displays six bands at 1688, 1669, 1615, 1565, 3282 and 3215 assigned to $\upsilon(C=O)_1$, $\upsilon(C=O)_2$ [11], $\upsilon(C=N)_1$, $\upsilon(C=N)_{ring}$ [12], $\upsilon(NH)_1$, $\upsilon(NH)_2$ [13], respectively.

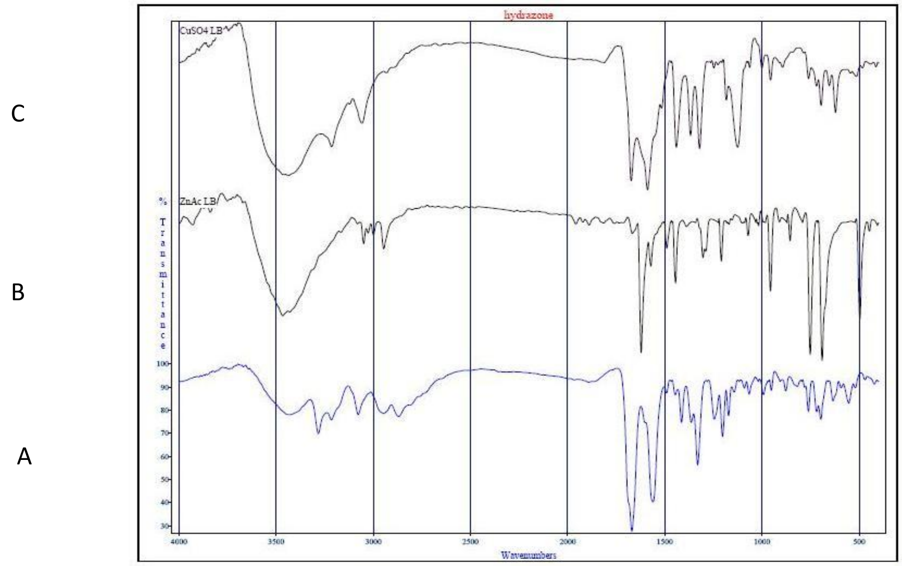

Fig. (2): IR spectra of (A) (H_2L), (B) $[[Zn(H_2L)(OAc)_2].H_2O$ and (C) $[Cu(H_2L)(SO_4)(H_2O)].H_2O$ complexes.

The ^1H NMR spectrum of H_2L in *DMSO* (Fig. 2) shows two signals at 11.54 and 11.44 ppm assignable to the protons of $(NH)_1$ and $(NH)_2$, respectively. The multiplet signals observed in the 7.31-8.7 ppm region are assigned to the aromatic protons and (N=C-H). The sharp singlet observed at 3.95 ppm is assigned to active methylene protons $(-CH_2)$.

In $[Zn(H_2L)(OAc)_2].H_2O$ and $[Pd(H_2L)Cl_2].2H_2O$ complexes, H_2L acts as a neutral bidentate ligand coordinating via two carbonyl oxygen groups $(C=O)_1$ and $(C=O)_2$. This mode of complexation is supported by the shift of $\upsilon(C=O)_1$ and $\upsilon(C=O)_2$ to lower wave numbers, the υ

$(NH)_1$, $\upsilon(NH)_2$, $\upsilon(C=N)_1$ and $\upsilon(C=N)_2$ vibrations remain more or less at the same position. Also, the IR spectra of these complexes show new bands at 495 and 514 cm^{-1} which may be attributed to υ(M-O) [14]. In addition, in the ^1H NMR spectrum of the $[Pd(H_2L)Cl_2].2H_2O$ complex, the signals attributed to the $\upsilon(NH)_1$ and $\upsilon(NH)_2$ protons appears at (10.97 and 9.08 ppm) indicating that these groups play no part in coordination.

Also, H_2L acts as a neutral tridentate ligand in $[Cu(H_2L)(SO_4)(H_2O)].H_2O$ complex, coordinating *via* carbonyl oxygen $(C=O)_1$, $(C=O)_2$ and azomethine nitrogen $(C=N)_1$. This mode of complexation is supported by the shift of $\upsilon(C=O)_1$, $\upsilon(C=O)_2$ and $\upsilon(C=N)_1$ to lower wave numbers, the $\upsilon(NH)_1$, $\upsilon(NH)_2$ and $\upsilon(C=N)_1$ vibrations remain nearly the same position. Also, the IR spectrum of this complex shows new bands at 514 and 440 cm^{-1} which may be attributed to υ(Cu-O) and υ(Cu-N) [15], respectively.

Moreover, H_2L acts as a monoegative tridentate ligand in $[Ni(HL)(OAc)H_2O].2H_2O$ and [Cd(HL)Cl] complexes, coordinating via carbonyl oxygen $(C=O)_2$, $\upsilon(C=N)_1$ and deprotonated enolized carbonyl oxygen $(=C-O^-)_1$. This mode of complexation is supported by; (i) the shift of both $\upsilon(C=N)_1$ and $\upsilon(C=O)_2$ to lower wave numbers, (ii) the disappearance of both $\upsilon(C=O)_1$ and $\upsilon(NH)_1$ with simultaneous appearance of new bands in 1624 and 1162-1166 cm^{-1} regions which assignable to $\upsilon(C=N^*)_1$and $\upsilon(C-O)_{1(enolic)}$ and (iii) the appearance of new band in 520-535 and 423-460 cm^{-1} which may be attributed to υ(M-O) and υ(M-N), respectively. The lack of signal due to $(NH)_1$ proton in the ^1H NMR spectrum of the diamagnetic Cd(II) complex emphasizes the deprotonation of the enolized carbonyl oxygen $(=C-O^-)_1$.

Finally, the IR spectra of $[CoL(H_2O)_3].H_2O$ and $[CuL(H_2O)_3].H_2O$ complexes reflect that the ligand acts as a binegative tridentate through azomethine nitrogen $(C=N)_1$ and two deprotonated enolized carbonyl oxygen groups $(=C-O^-)_1$, $(=C-O^-)_2$. This mode of complexation may be due to the disappearance of both $\upsilon(C=O)_1$, $\upsilon(C=O)_2$, $\upsilon(NH)_1$ and $\upsilon(NH)_2$ vibrations with simultaneous appearance of new bands in 1617, 1615,1166-1172 and 1112 cm^{-1} assignable to $\upsilon(C=N^*)_1$, $\upsilon(C=N^*)_2$, $\upsilon(C-O)_{1(enolic)}$ and $\upsilon(C-O)_{2(enolic)}$. The shift of $\upsilon(C=N)_1$ to lower wave numbers. Also, the IR spectra of these complexes show new bands in 510-516 and 450-470 cm^{-1} regions which may be attributed to υ(M-O) and υ(M-N), respectively.

In metal acetate complexes, the acetate group coordinates to the metal ions in a bidentate manner where the difference between the two acetate bands is $\Delta\nu \leq 180$ cm^{-1} **[**16]. Also, the bands of coordinated water observed at 854 and 595 cm^{-1}, are assigned to $\rho_r(H_2O)$ and $\rho_w(H_2O)$, respectively [16]. Moreover, strong evidence for the presence or absence of water of crystallization and/or coordinated water supported by the thermogram of all complexes.

Electronic spectra and magnetic moment measurements

The electronic spectrum of $[Ni(HL)(OAc)H_2O].2H_2O$ complex shows two bands at 15385 and 25000 cm^{-1} regions attributed to $^3A_{2g} \rightarrow {}^3T_{1g}(F)$ and $^3A_{2g} \rightarrow {}^3T_{1g}(P)$ transitions, respectively, in an octahedral geometry [17]. The calculated values of D_q, B, β and υ_2/υ_1 lie in the range reported for an octahedral structure. The position of υ_1 (9616 cm^{-1}) is calculate theoretically [17]. Also, the magnetic moment value (μ_{eff}=3.2 B.M.) is additional evidence for an octahedral geometry.

Table (3): Magnetic moments, electronic spectra and ligand field parameters of metal complexes of H_2L

Compound	$\mu_{eff.}$ (B.M.)	Band position (cm^{-1})	D_q (cm^{-1})	B (cm^{-1})	β	υ_2/υ_1
$[Ni (HL)(OAc)H_2O].2H_2O$	3.2	15385; 25000	1177	336	0.35	1.6
$[Co(L)(H_2O)_3].H_2O$	5.2	14286; 17606	758	798	0.82	2.1
$[Cu(H_2L)(SO_4)(H_2O)].H_2O$	1.8	14285; 16894	-	-	-	-
$[Cu(L)(H_2O)_3]. H_2O$	2.1	14492; 16949	-	-	-	-

The magnetic moments, electronic spectral bands in *DMSO* and ligand field parameters of metal complexes are collected in Table 3.

The electronic spectrum of $[Co(L)(H_2O)_3].H_2O$ complex shows two bands at 14286 and17606 cm^{-1} attributed to $^4T_{1g} \rightarrow {}^4A_{2g}(F)$ and $^4T_{1g} \rightarrow {}^4T_{1g}(P)$ transitions, respectively, in an octahedral configuration. The calculated D_q, B, β and υ_2/υ_1 values are in the range reported for an octahedral environment around Co(II) ion [17]. The position of υ_1 (6803 cm^{-1}) is calculate theoretically [17]. Also, the value of the magnetic moments (5.2 B.M.) is consistent with octahedral structure.

The copper(II) complexes have magnetic moment values (1.8-2.1 B.M.), indicating the presence of Cu^{2+} ion. The electronic spectra of both $[Cu(H_2L)(SO_4)(H_2O)].H_2O$ and $[Cu(L)(H_2O)_3].2H_2O$ complexes show a broad band in the 16894-16949 cm^{-1} region with a shoulder in the 14285-14492 cm^{-1} region which may be assigned to $^2B_{1g} \rightarrow {}^2E_g$ and $^2B_{1g} \rightarrow {}^2A_{1g}$ transitions, respectively, in a tetragonally distorted octahedral configuration [18].

Thermal analysis

The TG curves of $[Ni(HL)(OAc)(H_2O)].2H_2O$ complex displays 7.8% weight loss in the temperature range 40-160 °C which correlated to two water molecules outside the coordination sphere. In the temperature range 160-275 °C, the TG curves exhibits 17.0% weight loss which could be ascribed to the elimination of the one coordinating water molecules [19] as well as the acetate group [20]. Thermal degradation of the organic molecule starts above 275 °C. Over the temperature 275-322 °C, the weight loss 21.6% in the TG curve is most probably ascribed to the partial decomposition of the chelating agent with the elimination of the loosely bound ($C_3H_3N_2S$) moiety. The final weight loss of 37.3% ending at 640 °C, is largely attributed to complete decomposition of the organic molecule, alongside rupture of the chelate bond, leaving NiO comprising 16.3% of the initial mass of the complex.

Table (4): Thermal behavior of metal complexes of H_2L

Compound (Molecular weight)	Temp. Range, (°C)	Decomposition product(s) loss (Formula weight)	Weight % Found (Calcd)
$[Cu(L)(H_2O)_3] .H_2O$ $CuC_{13}H_{18}O_6N_4S$ (421.787)	40-120	H_2O (18.015)	4.3(4.3)
	120-240	$3\ H_2O$ (54.045)	12.8(12.8)
	240-340	C_3H_2NS (84.120)	19.9(19.9)
	340-665	$C_{10}H_8N_3O$ (186.195)	44.1(44.1)
	>665	Residue; CuO (79.54)	18.9(18.9)
$[Ni(HL)(OAc)H_2O].2H_2O$ $NiC_{15}H_{20}O_7N_4S$ (458.995)	40-160	$2H_2O$ (36.03)	7.8 (7.8)
	160-275	$H_2O + CH_3COOH$ (78.068)	17.0 (17.0)
	275-322	$C_3H_3N_2S$ (99.134)	21.6(21.6)
	322-640	$C_{10}H_7N_2O$ (171.180)	37.3(37.3)
	>640	Residue; NiO (74.71)	16.3(16.3)

The TG curves of $[Cu(L)(H_2O)_3].H_2O$ complex displays 4.3% weight loss in the temperature range 40-120°C which correlated to water of crystallization. In the temperature range 120-240 °C, the TG curves exhibits 12.8% weight loss which could be ascribed to the elimination of the three coordinating water molecules [19]. In the temperature range 240-340 °C, the TG curves displays 19.9% weight loss which could be corresponding to the loosely bound(C_3H_2NS) moiety. Thermal degradation of the remaining organic molecule starts above 340 °C. Over the temperature range 340-665 °C, the weight loss 44.1% in the TG curve is most probably assigned to the elimination of the loosely bound($C_{10}H_8N_3O$) moiety. The final weight loss of 44.1% ending at 665 °C, is attributed to complete decomposition of the remaining more tightly bound fragment of the organic molecule, alongside rupture of the chelate bond, leaving CuO comprising 18.9% of the initial mass of the complex (Table 4).

Kinetic data

The kinetic and thermodynamic parameters of thermal degradation process have been calculated using Coats-Redfern and Horowitz-Metzger models [21]. Coats-Redfern relation is as follows:

$$\ln[-\frac{\ln(1-\alpha)}{T^2}] = \ln\left(\frac{AR}{\beta E}\right) - \frac{E}{RT} \qquad (1)$$

Where α represents the fraction of sample decomposed at time t, defined by: $\alpha = \frac{w_o - w_t}{w_o - w_\infty}$, wo, wt and w∞ are the weight of the sample before the degradation, at temperature t and after total conversion, respectively. T is the derivative peak temperature. β is the heating rate = dT/dt, E and A are the activation energy and the Arrhenius pre-exponential factor, respectively. A plot of $\ln[-\frac{\ln(1-\alpha)}{T^2}]$ versus 1/T gives a straight line whose slope (E/R) and the pre-exponential factor (A) can be determined from the intercept.

A number of pyrolysis processes can be represented as a first order reaction. Particularly, the degradation of a series of H_2L complexes was suggested to be first order [22], therefore we assume n = 1 for the remainder of the present text. The other thermodynamic parameters of activation can be calculated by Eyring equation [23]:

$$\Delta H = E - RT \qquad (3)$$

$$\Delta S = R \ln \frac{hA}{k_B T} \qquad (4)$$

$$\Delta G = \Delta H - T\Delta S \qquad (5)$$

Table (5): Kinetic and thermodynamic Parameters of complexes evaluated by Coats-Redfern equation.

Complex	peak	Mid Temp(K)	Ea KJ\mol	A (S^{-1})	ΔH* KJ\mol	ΔS* KJ\mol.K	ΔG* KJ\mol
$[Cu(L)(H_2O)_3].H_2O$	1st	356	60.782	17205.246	57.823	-165.300	116.670
	2nd	450	87.242	67073.870	83.517	-155.899	153.360
	3rd	563	131.580	7.47898E6	126.899	-118.606	193.675
	4rd	775	156.784	11079.717	149.617	-176.311	301.598
$[Ni(HL)(OAc)H_2O].2H_2O$	1st	371	26.424	44.837	23.339	-215.111	103.146
	2nd	488	37.418	43.810	33.360	-217.582	139.541
	3rd	572	215.346	1.14737E14	210.133	18.062	198.809
	4rd	754	419.033	2.54098E24	412.282	213.959	238.547

Thermodynamic parameters such as activation energy (Ea), pre-exponential factor(A), entropy of activation (ΔS), enthalpy of activation (ΔH) and free energy of activation (ΔG) of decomposition steps were calculated using Coats - Redfern [21] (Tables 5). In this method, the lift side of equations 3 and 4 are plotted against 1/T (Figs. 3, 4). From the results, the following remarks can be pointed out:

- The high values of the energy of activation, E of the complexes reveals the high stability of such chelates due to their covalent bond character [24].
- The positive sign of ΔG for the investigated complexes reveals that the free energy of the final residue is higher than that of the initial compound, and all the decomposition steps are non-spontaneous processes. Also, the values of the activation, ΔG increases significantly for the subsequent decomposition stages of a given complex. This is due to increasing the values of TΔS significantly from one step to another which overrides the values of ΔH [25- 27].
- The negative values of ΔS for the degradation process indicates more ordered activated complex than the reactants or the reaction is slow [23].

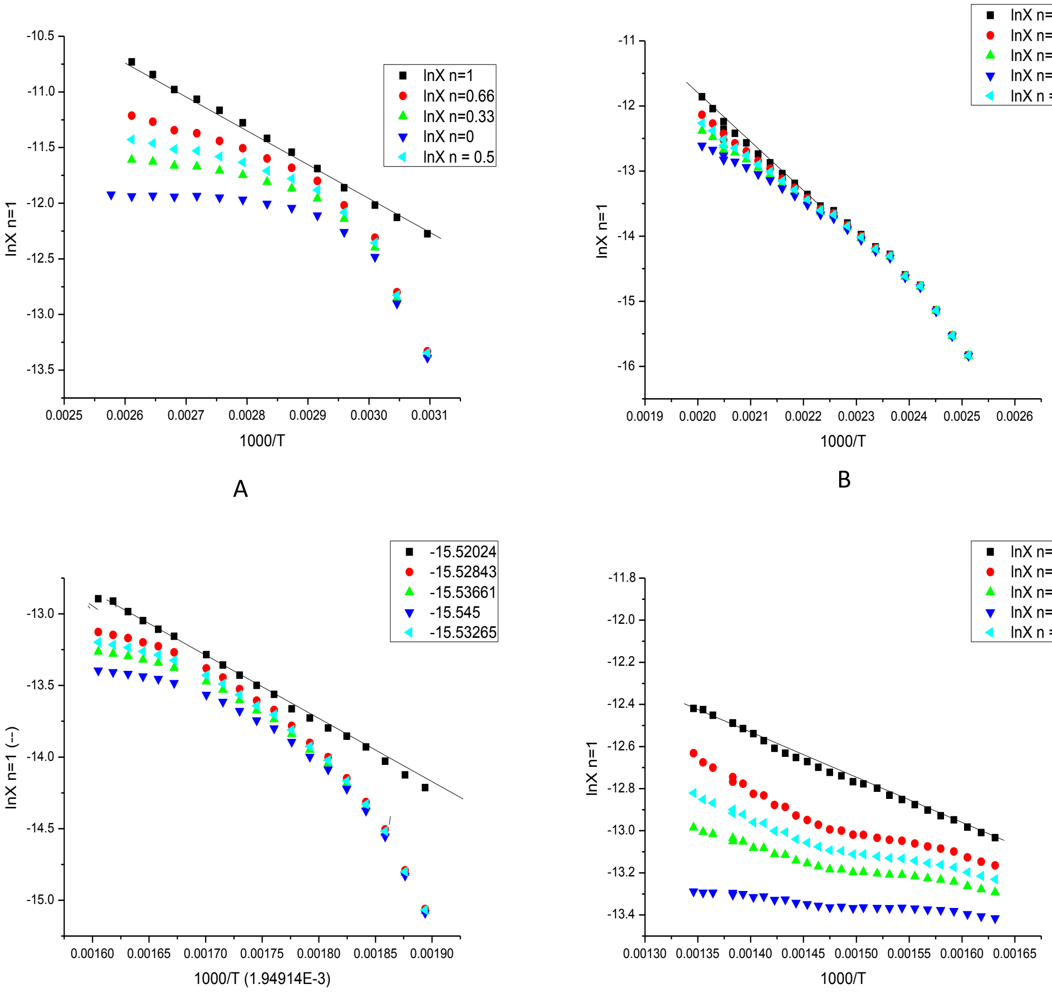

A

B

C

D

Fig. (3): Coats-Redfern plots of (A) step(1), (B) step(2), (C) step(3) (D) step(4) of $[Cu(L)(H_2O)_3].H_2O$

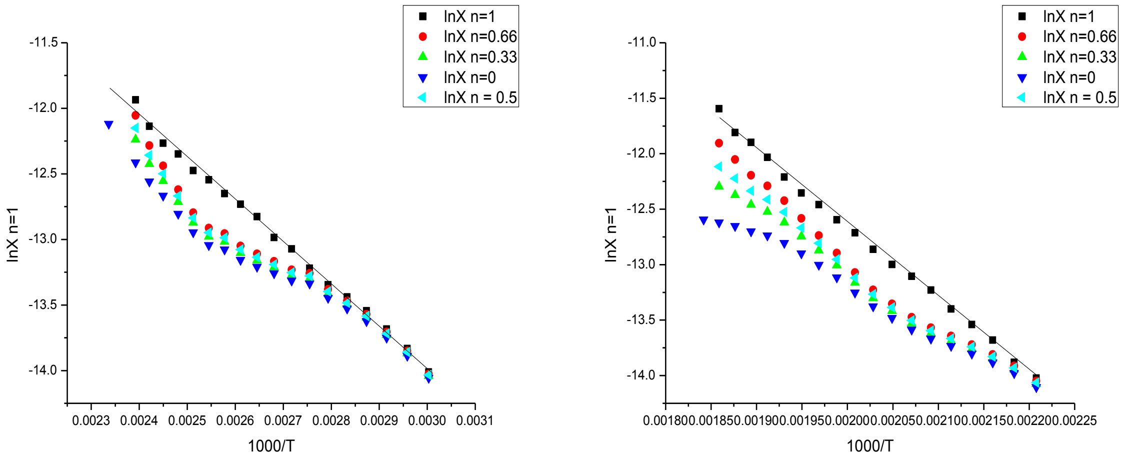

A

B

B

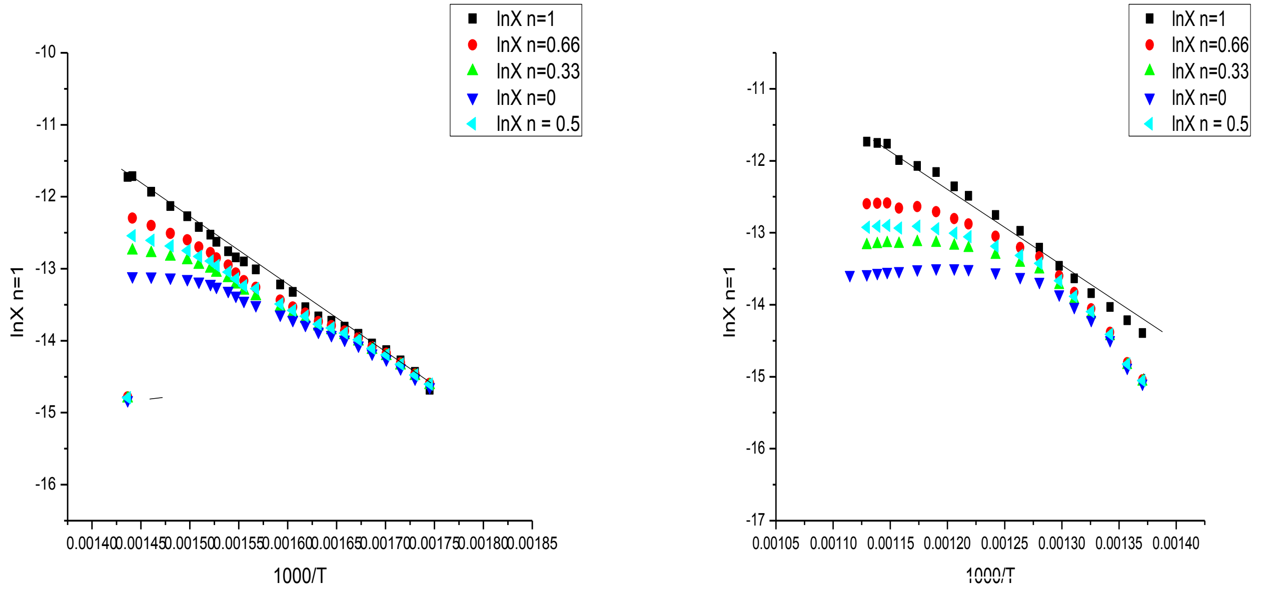

C

D

Fig. (4): Coats-Redfern plots of (A) step(1), (B) step(2), (C) step(3) (D) step(4) of [Ni(HL)(OAc)(H_2O)].$2H_2O$

Biological Activity

The reported high biological activity of hydrazones have prompted us to undertake systematic studies on their complexation tendency and test their efficacies and potencies against economically important antifungal such as *Aspergillus sp.* and *Stemphylium sp.* Also, bacteria such as *B. Subtillis* and *P. Aeurginosa* [28].

Antifungal activity

Table (6): Antifungal activity of the (H_2L) ligand and its metal complexes

Compound	% Inhibition of spore germination					
	Aspergillus sp (mg/ml)			*Stemphylium sp.* (mg/ml)		
	0.5	1.0	1.5	0.5	1.0	1.5
Miconazole (standard)	62	80	90	52	70	90
H_2L	34	45	73	41	55	62
[Zn(H_2L)($OAc)_2$].H_2O	65	80	85	60	83	90
[Pd(H_2L)Cl_2].$2H_2O$	70	87	96	54	76	94
[Cd(HL)Cl].H_2O	70	85	96	60	80	94
[Ni(HL)(OAc)H_2O].$2H_2O$	49	55	74	52	69	85
[Co(L)($H_2O)_3$].H_2O	47	55	69	50	72	85
[Cu(L)($H_2O)_3$].H_2O	60	70	82	59	75	88

The experimental antifungal activity data (Table 6) indicate that the ligand as well as its complexes shows an appreciable activity against *Aspergillus sp.* and *Stemphylium sp.* at 0.5, 1.0

and 1.5 mg/ml concentration. Their activity generally increases with increasing the concentration of the compounds. *DMSO* control has shown a negligible activity as compare to the ligand and its metal complexes. The experimental results of the compounds were compared against *DMSO* as the control and are expressed as percentage inhibition versus control. The complexes are more effective against *Aspergillus sp.* than *Stemphylium sp.* $[Pd(H_2L)Cl_2].2H_2O$ and $[Cd(HL)Cl].H_2O$ shows the highest activity (96%) against *Aspergillus sp.* at the concentration of 1.5 mg/ml among all the metal complexes. The same complex also shows the highest activity (94%) against *Stemphylium sp.* The antifungal activity varies in the following order of fungal species:

Aspergillus sp. > Stemphylium sp.

All the metal complexes exhibited greater antifungal activity against *Aspergillus sp.* as compare to the standard drug *Miconazole*. The Ni(II), Co(II), Cu(II), Cd(II), Zn(II) and Pd(II) complexes show better activity against *Stemphylium sp.* than *Trichoderma sp.* whereas, Pd(II) and Cd(II) complexes are more effective. From the data it has also been observed that the complexes are more active than the ligand [29]. The toxicity of the complexes can be related to the strength of the metal-ligand bond, besides other factors such as size of the cation [30], receptor sites, diffusion and a combined effect of the metal and ligand [31] for inactivation of the biomolecules.

Antibacterial activity

Table (7): Antibacterial activity of the (H_2L) ligand and its metal complexes

Compound	% Inhibition of spore germination					
	E. coli (mg/ml)			*Clostridium sp.* (mg/ml)		
	0.5	1.0	1.5	0.5	1.0	1.5
Miconazole (standard)	70	85	100	60	70	95
H_2L	44	62	69	40	58	77
$[Zn(H_2L)(OAc)_2].H_2O$	70	83	91	59	75	90
$[Pd(H_2L)Cl_2].2H_2O$	78	85	98	65	75	95
$[Cd(HL)Cl].H_2O$	76	80	98	60	71	95
$[Ni(HL)(OAc)H_2O].2H_2O$	45	60	75	45	60	70
$[Co(L)(H_2O)_3].H_2O$	44	63	77	44	63	75
$[Cu(L)(H_2O)_3].H_2O$	66	75	86	66	75	83

The metal complexes, ligand, standard drug *Ampicillin* and *DMSO* solvent control were screened separately for their antibacterial activity against *E. coli* and *Clostridium sp.* at 0.5, 1.0 and 1.5 mg/ml concentration. Their activity is greatly enhanced at the higher concentration [32]. The activity of the complexes has been compared with the activity of a common standard antibiotic *Ampicillin*. The antibacterial results suggest that the ligands and their complexes (Table 7) show a moderate activity against both the bacteria [33, 34] as compared to the standard drug (*Ampicillin*). The metal complexes show higher antibacterial activity than the ligands. The *DMSO* control showed no activity against any bacterial strain.

REFERENCES

[1] Özmen ÜÖ, Olgun G. Spectrochim Acta Part A 2009;70: 641–5.

[2] Avaji PG, Kumar CHV, Patil SA, Shivananda KN, Nagaraju C. Eur J Med Chem 2009;44: 3552–9.

[3] Zang Y, Zang L, Liu L, Guo J, Wu D, Xu G, Wang X Jia D. Inorg Chim Actam 2010; 363: 289-93.

[4] Lima LM, Frattani FS, dos Santos JL, Castro HC, Fraga CAM, Zingali RB, Barreiro EJ. Eur J Med Chem 2008; 43: 348-56.

[5] Seleem HS, El-Inany GA, Mousa M, Hanafy FI. Spectrochim Acta Part A 2009; 74: 869-74.

[6] Singh VP. Spectrochim Acta Part A 2008; 71:17-22.

[7] Khalifa ME. Anal Fr 1995; 23: 453.

[8] Shoukry AA, Shoukry MM. Spectrochim Acta Part A 2008; 70:686-91.

[9] Madrakian T, Afkhami A, Mousavi A. Talanta 2007; 71:610-4.

[10] Vogel AI. Quantitative Inorganic Analysis, Longman, London, 1989.

[11] Ibrahium KM, Rakaha TH, Abdalla AM, Hassanian MM. J Indian Chem 1993; 32: 361-3.

[12] Guzar SH. J I N Qin-han J Applied Sci b2008; 8: 2480-5.

[13] Narang KK, Singh VP. Trans Met Chem 1996; 21: 507-11.

[14] Nakamoto K. Infrared spectra of inorganic coordination compounds, Wiley Interscience, New York, 1970.

[15] Pyta K, Przybylski P, Huczyn´ski A, Hoser A, Woz´niak K, Schilf W, Kamien´ski B, Eugeniusz Grech D. J Mol Struct 2010; 970: 147-54.

[16] Al-Hazmi GAA, El-Shahawi MS , Gabr IM , El-Asmy AA. J Coord Chem 2005; 58: 713-33.

[17] Lever ABP. Inorganic Electronic Spectroscopy Elsevie Amsterdam 1968.

[18] Ayman AH, J Appl Sci Res 2007; 3(12): 1663-70.

[19] Warad DU, Statish CD, Kulkarni VH, Bajgur CS. Ind J Chem 2000; 39: 415-20.

[20] Rakha TH, Ibrahim KM, Khalifa ME. Thermochim Acta 1989;144: 53-63.

[21] Coats AW, Redfern JP. Nature 1964; 20: 68-9.

[22] Broido A. J Ploym Sci A-2 1969:7: 1761-73.

[23] Frost AA, Pearson RG. Kinetics and Mechanisms Wiley New York, 1961.

[24] Taakeyama T, Quinn FX. Thermal Analysis Fundamentals and Applications to Polymer Science, Joh Wiley and Sons, Chichester, 1994.

[25] Maravalli PB, Goudar TR. Thermochima Acta 1999;325: 35-41.

[26] Yusuff KKM Sreekala R. Thermochima Acta 1990;159:357-68.

[27] Kandil SS, El-Hefnawy GB, Baker EA. Thermochim Acta 2004; 414: 105-13.

[28] Filippovic N, Borrmann H, Todorovic T, Borna M, Spasojevic V, Sladic D, Novakovic I, Andjelkovic K. Inorg Chim Act 2009; 362: 1996-2000

[29] Thimmaiah KN, Chandrappa GT, Rangaswamy, Jayarama. Polyhedron 1984; 3: 1237–39.

[30] Nagar R. J Inorg Biochem 1990; 40: 349–56.

[31] Johari RB, Sharma RC. J Indian Chem Soc 1988; 65: 793- 94.

[32] Abd El-Wahab ZH, El-Sarrag MR. Spectrochim. Acta A 2004: 60: 271–77.

[33] Deepa K, Aravindakshan KK. Synth React Inorg Met Org Nano Met Chem 2005; 35: 409–16.

[34] Panchal PK, Parekh HM, Patel MN. Toxicol Environ Chem 2005; 87: 313-20.